Click Here for Full Article

Variability of Pacific subtropical cells in the 50-year ECCO assimilation

Friedrich A. Schott,[1] Weiqiang Wang,[1] and Detlef Stammer[2]

[1] The Pacific Subtropical Cell (STC) circulation is being analyzed from transport time series across 9°S and 9°N, obtained from the German ECCO (GECCO) assimilation results for the period 1952–2002. In this estimate, the interior Pacific STC convergence shows significantly less decadal slowdown from the 1960's to the 1990's (~5Sv), than in previous estimates based on hydrographic sections. In the GECCO results, about half of this STC convergence decrease is compensated by an increase in the equatorward transport of the western boundary currents. Overall, the STC varies primarily on interannual time scale, with relatively short time lags between STC convergence and transport variations of the Equatorial Undercurrent at 140°W. **Citation:** Schott, F. A., W. Wang, and D. Stammer (2007), Variability of Pacific subtropical cells in the 50-year ECCO assimilation, *Geophys. Res. Lett.*, *34*, L05604, doi:10.1029/2006GL028478.

1. Introduction

[2] The subtropical cells are shallow overturning cells connecting the subtropics with the equatorial regimes of the Pacific and Atlantic Oceans [*McCreary and Lu*, 1994; *Malanotte-Rizzoli et al.*, 2000; *Schott et al.*, 2004]. Water masses that are subducted into the thermocline in the eastern subtropics of both hemispheres are swept westward by the North and South Equatorial Currents, respectively (Figure 1a). They can reach the equator either via western boundary undercurrents or by meridional pathways in the interior. For the variability of the STC transports, *McPhaden and Zhang* [2002] (referred to as MPZ hereafter) reported a drastic decadal decrease of the interior equatorward STC convergence across 9°N/9°S, by about 12 Sv, from the mid-1950s to the mid-1990s. This decrease of STC convergence was accompanied by warming of the upwelled equatorial water, in agreement with the concept of decreased STC activity. Subsequently, *McPhaden and Zhang* [2004] found an increase of STC convergence again from the 1990's into the time period 2001–2004, which was accompanied by cooling of equatorial upwelling waters.

[3] Since the MPZ calculation was based on geostrophy (referenced to 900 m), applied to available hydrographic measurements along two zonal sections, an evaluation of the wider observational data base is of interest. In particular, the role of the boundary currents in relation to the STC variability diagnosed for the interior ocean needs further investigations. However, the observational data base is insufficient for determining STC transport time series. One possibility to address this question is to analyze the output from a numerical model that was constrained, in a dynamically consistent way, by most available hydrographic data such as the observations used by MPZ, in addition to altimetric sea level data, sea surface temperature and atmospheric forcing fields. We use here results available from the German contribution (henceforth called GECCO) to the Estimating the Climate and Circulation of the Ocean (ECCO) assimilation effort [*Stammer et al.*, 2002, 2004] for determining STC transports of the model for the time period studied by MPZ. One obvious difference of our analysis to the evaluation of MPZ is that their analysis was confined to observations available along the two sections, 9°N and 9°S, whereas the assimilation results are influenced by the entire suite of observations available over the Pacific Ocean and globally, including those available from the equatorward thermocline and poleward near-surface flow fields as well as from the Equatorial Undercurrent (EUC).

2. The 50-Year GECCO Assimilation

[4] The output fields analyzed here were obtained from the 50-year GECCO run covering the period 1952–2002. The run is based on, and is extending, the earlier global ECCO estimate on a 1° global grid and 23 depth levels which is described in detail by *Stammer et al.* [2004] and *Köhl et al.* [2006]. As before (in the shorter run) the ECCO/MIT model is applied here again which uses the model's adjoint to constrain the solution in a dynamically self-consistent way by most available hydrographic, sea surface height and other data, as well as surface flux fields available since the beginning of the 1950s. The model is being brought into consistency with available observations and their uncertainties by changing the initial temperature and salinity fields and by adjusting the time varying surface forcing (the initial forcing is the NCEP twice-daily wind stress, and daily heat and freshwater flux). The data constraints after 1992 agree with those used by *Köhl et al.* [2006]. Further details on the optimization are provided by *Köhl et al.* [2006, 2007].

[5] For a comparison with the GECCO results, we also evaluate those model fields available from the unconstrained GECCO run, i.e. the same model version except that no data were assimilated, and Levitus initial temperature and salinity conditions and NCEP forcing were used (including a surface relaxation term). This run will be referred to in the following as the GECCO reference run. Time series shown below were filtered using a 25-month Hanning filter to eliminate the seasonal and other short-

[1]Leibniz-Institut für Meereswissenschaften (IFM-GEOMAR), Kiel, Germany.
[2]Institut für Meereskunde, Zentrum für Marine und Atmosphärische Wissenschaften, Universität Hamburg, Hamburg, Germany.
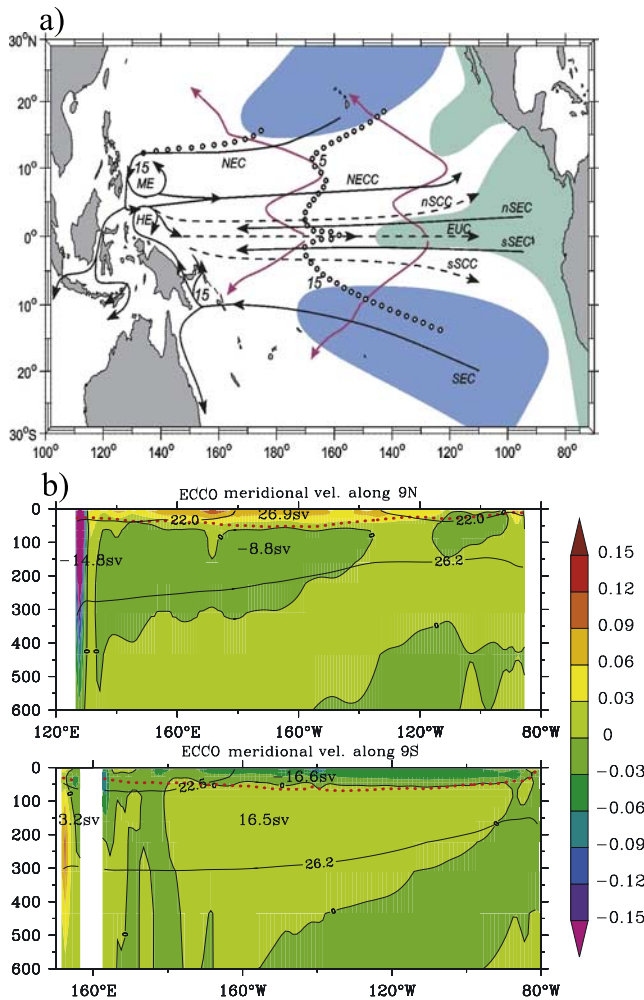
Figure 1. (a) Schematic representation of the Pacific circulation branches, subtropical subduction zones and equatorial/eastern upwelling regimes that participate in the STC. Current branches are NEC = North Equatorial Current; nSEC, sSEC = South Equatorial Current north and south of the equator; NECC = North Equatorial Countercurrent; EUC = Equatorial Undercurrent; NSCC, SSCC = North and South Subsurface Countercurrent. Interior equatorward thermocline pathways dotted, equatorward transport estimates (in Sv = 10^6 m^3 s^{-1}) marked; selected surface poleward drifter pathways for the central basin marked by thin lines; see text for details (adapted from *Schott et al.* [2004]). (b) Mean sections of meridional velocity across (top) 9°N and (bottom) 9°S from GECCO with isopycnals (in kgm^{-3}) marking the upper and lower boundary of the STC layer; also marked are the bottom of the mixed-layer (dotted line) and transports (in Sv) of the mixed layer and STC layer (separately for interior and western boundary).

period variability not of interest here. The standard deviations listed were computed from those smoothed time series.

3. The Mean STC Circulation in GECCO

3.1. The 9°N and 9°S Section Transports

[6] Using similar isopycnals as MPZ to mark the top and bottom of the STC layer, mean equatorward transports for

the interior STC branches of -8.8 ± 2.9 Sv across 9°N (from 145°–80°W and in 22.0–26.2 kgm^{-3} density range) and of 16.5 ± 2.4 Sv across 9°S (from 160°–80°W and in 22.5–26.2 kgm^{-3} density range) are obtained, yielding an interior STC convergence of 25.3 ± 4.6 Sv. The 9°S value is quite similar to the earlier estimates summarized by *Schott et al.* [2004], the 9°N value is higher. The geostrophic transport relative to 900 m (for compatibility with computations from MPZ) yields -6.1 ± 2.0 Sv across 9°N and 11.7 ± 1.8 Sv across 9°S (which is much lower than the absolute value; see also the offset in Figure 2a), and a convergence of 17.8 ± 3.2 Sv. The western-boundary current (wbc) contributes -14.8 ± 2.0 Sv to the STCs across 9°N (Figure 2a), which is comparable to estimates obtained from observations, while at 9°S the wbc contribution of 3.2 ± 1.2 Sv to the STC is much lower than estimates based on observations.

### 3.2. Mixed-Layer and Ekman Transports Across 9°N and 9°S

[7] The interior mixed-layer transports are poleward, at 26.9 ± 2.1 Sv for 9°N and -16.6 ± 1.5 Sv for 9°S, yielding a divergence of 43.5 ± 2.8 Sv. Subtracting from these the equatorward geostrophic (rel. to 900 m) transports of -6.4 ± 1.5 Sv and 12.8 ± 2.7 Sv across 9°N and 9°S, respectively, provides non-geostrophic transports of 33.3 ± 2.5 Sv across 9°N and 29.4 ± 3.2 Sv across 9°S. They are in very close agreement with the mean Ekman transports from GECCO wind stresses, which amount to 35.2 ± 2.6 Sv at 9°N and -30.0 ± 3.5 Sv at 9°S.

4. STC variability

4.1. STC Transports Across 9°N and 9°S

[8] The GECCO transports in the interior thermocline layers across 9°N and 9°S (from the monthly output fields) show strong seasonal to interannual variations but relatively low decadal changes (Figure 2a). Also shown are the geostrophic STC transports, relative to 900 m for comparison with the low-passed absolute transports. The curves differ more at 9°S than at 9°N as mentioned above, indicating some role of mean reference currents (Figure 2a). Nevertheless, the variability of both transport estimates agree reasonably well for the most part of the 50-year period.

[9] In Figures 2b and 2c the low-passed variability of the interior STC transport is compared with the western-boundary contributions of the STC and the coast-to coast total STC transport. Two results are obvious. First, there are no striking decadal trends apparent, neither in the interior, nor for the wbc or total STC transports. Second, at the interannual time scale, interior transport anomalies are in many instances compensated, in part or in total, by wbc anomalies of opposite sign. The correlation therefore shows anti-phase between the interior and the wbc STC. Overall, the interior STC variance is larger than that of the wbc, in particular at the 9°S section. Since we are doubtful of GECCO trends in the first 5–10 years, finding that the Indonesian Through-flow and Atlantic MOC show strong initial changes in GECCO, we compare in the following the time periods 1990–99 against 1962–71 (Table 1) to document decadal changes.
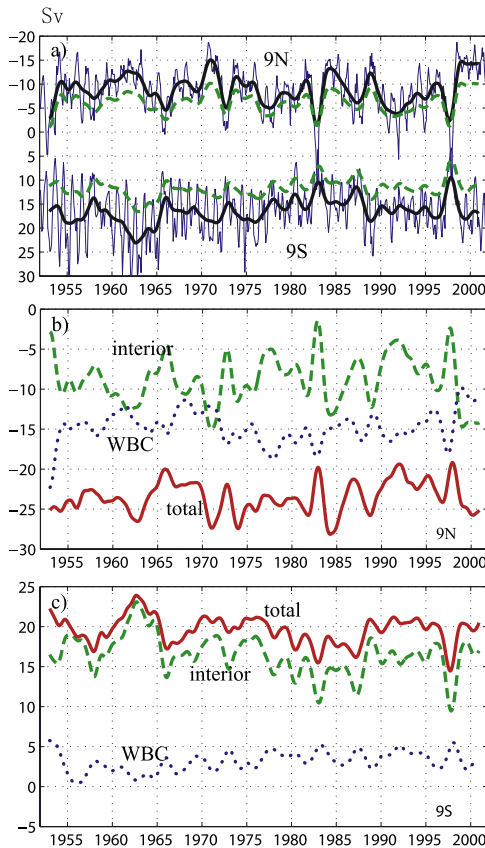
Figure 2. (a) Time series of monthly (thin solid line) and low-pass (25 month Hanning) filtered (heavy solid line) STC-layer transports for Pacific interior, integrated in 22.0–26.2 kgm^{-3} density range from 145°–80°W along 9°N and from 160°E–80°W along 9°S; also shown are low-passed geostrophic (rel. 900 m) transports (heavy dashed line), (b) low-pass filtered time series of interior (dashed line), wbc (dotted line) and coast-to coast (solid line) STC transports across 9°N, (c) as in Figure 2b but for 9°S.

4.2. STC Convergence and EUC

[10] There is a slight decadal decrease of the interior STC strength at 9°N and 9°S (Figure 3a), but at both latitudes the wbc averages increase over the decades. The net result is a total decrease by 4.8 ± 6.0 Sv of the interior STC convergence from the 1962–71 time period to the 1990–1999 period (Figure 3b; Table 1). This is partially compensated by an increase of the wbc STC convergence of 2.5 ± 2.2 Sv, such that there is only a net decrease of the coast-to-coast STC transport of 2.3 Sv over the 30-year time period. In comparison, the interior geostrophic STC transports rel. 900 m (Figure 3b) shows an even smaller interior decline of only 3.0 ± 4.3 Sv between the 1960s and the 1990s (Table 1). This small decadal decrease differs substantially from the interior geostrophic STC transport divergence derived by MPZ from evaluating historical data along 9°N and 9°S (Figure 3b).

[11] When comparing the EUC at 140°W with the interior STC convergence variability (Figure 4a) obvious relations between both are apparent at interannual time scales. Typically, a decrease of the interior STC transports at both latitudes will lead to a decreased EUC transport a

few months later. Maximum correlation with interior STC convergence occurs at 5–6 months lag of the EUC. The mechanism for this fast time scale, which was also found in a model analysis by *Cheng et al.* [2007] for the EUC/STC variability during the 1990s, still needs to be explored. At the decadal timescale the EUC decreases by 4.7 ± 3.3 Sv from the 1960s to the 1990s (Table 1), very similar to the interior STC decrease (Table 1). However, including the wbc increase of 2.5 ± 2.2 Sv, the EUC is decreasing more strongly than the total STC convergence. The Indonesian Throughflow stays almost constant for the isopycnal range of the STCs (Figure 4a). The cause of the STC decrease appears to be the Ekman divergence, which decreases by 6.1 ± 3.5 Sv from the 1960s to the 1990s, and equatorial upwelling corresponds with a decrease of 7.3 ± 2.4 Sv across the 100 m level east of 140°W, and in the 3°S–3°N band (Table 1). The reduced upwelling is accompanied by a decadal warming of 0.6°C.

4.3. Comparison With the Unconstrained Reference Run

[12] GECCO is initially forced by the NCEP wind stresses, and NCEP is known to have a large decadal trend in the Pacific near-equatorial zonal winds [*Alory et al.*, 2005]. The 9°N°/9°S Ekman divergence from NCEP decreases from 70 Sv in the 1950's to below 50 Sv in the 1990's (Figure 4b). A relatively large decline also existed in a mean of four wind stress products that MPZ evaluated for 9°N°/9°S Ekman transport estimates. It is now interesting to note that in the forcing fields estimated through the GECCO assimilation, this multidecadal trend in the Ekman divergence almost disappears (Figure 4b). (The drift constraints
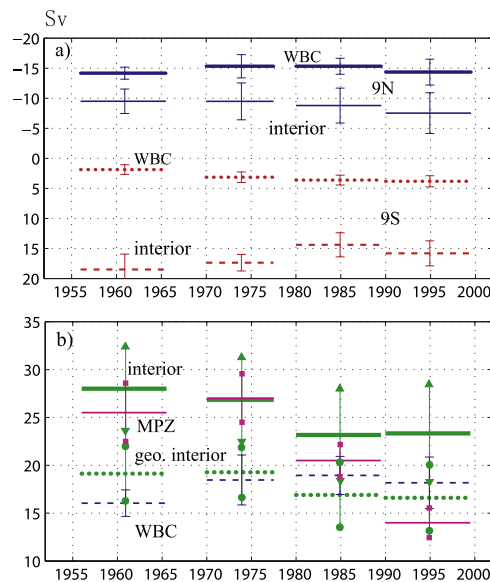
Figure 3. (a) STC transports with std. deviations, for selected time segments, for interior (across 9°N, thin solid line; across 9°S, dashed line) and for wbc (across 9°N, heavy solid line; across 9°S, dotted line) contributions, (b) STC transport convergence for 9°N/9°S sections for interior (heavy solid line) and wbc (dashed line); also shown is interior geostrophic STC transport convergence from GECCO (dotted line) and from MPZ (thin solid line).

Table 1. Transports of STC Elements for Time Periods 1962–71 (P1) and 1990–99 (P2) in the GECCO Assimilation and the Reference Run[a]

| | | 1962–1971(P1) | | 1990–1999(P2) | | |
		9N	9S	9N	9S	Diff. (P2-P1)
WBC	assim	−13.5 ± 1.3	2.2 ± 0.9	−14.4 ± 2.2	3.8 ± 0.9	
interior	assim	−9.9 ± 2.7	18.2 ± 2.5	−7.5 ± 3.4	15.8 ± 2.1	
total	assim	−23.3 ± 2.2	20.0 ± 1.7	−21.9 ± 1.6	21.4 ± 1.8	
interior conv.	assim	28.1 ± 4.5		23.3 ± 4.8		−4.8 ± 6.0
	geostr	*19.6 ± 3.0*		*16.6 ± 3.4*		*−3.0 ± 4.3*
	ref	25.1 ± 4.8		14.7 ± 3.3		−10.6 ± 5.3
WBC conv.	assim	15.7 ± 1.4		18.2 ± 2.7		2.5 ± 2.2
	ref	20.3 ± 2.2		22.4 ± 2.3		2.1 ± 1.8
EUC	assim	17.7 ± 2.5		13.0 ± 3.2		−4.7 ± 3.3
	ref	17.7 ± 3.3		10.9 ± 3.0		−6.8 ± 3.5
ITF	assim	−6.4 ± 1.0		−7.0 ± 0.8		−0.6 ± 1.5
	ref	−7.0 ± 0.8		−5.0 ± 0.8		2.1 ± 0.9
Ekm div.	assim	67.1 ± 3.9		61.0 ± 2.8		−6.1 ± 3.5
	ref	61.8 ± 4.4		45.9 ± 2.4		−15.9 ± 4.0
ML div.	assim	44.2 ± 2.5		41.5 ± 2.4		−2.7 ± 2.6
	ref	42.8 ± 2.6		35.5 ± 2.1		−7.3 ± 2.8
SST(°C)[b]	assim	25.0 ± 0.5		25.6 ± 0.8		0.6 ± 0.8
Upwelling[b]	assim	23.3 ± 2.0		16.0 ± 2.1		−7.3 ± 2.4

[a]Unit: Sv.
[b]Upwelling transport across 100m for 3S-3N and 140W-80W.

applied to the GECCO optimization do not prevent the adequate fit to the data; see the extensive discussion by *Köhl et al.* [2006]).

[13] In the GECCO reference run, i.e., the same model with NCEP forcing, the interior STC convergence shows a large decadal decrease (Figure 4b), of 10.6 ± 5.3 Sv from 1962–71 to 1990–99, more than double the decrease resulting from GECCO (Table 1) and of the same magnitude as the STC changes reported by MPZ. The wbc contribution to the decadal STC convergence is small in the reference run, yielding only an increase by 2.1 ± 1.8 Sv between both periods, similar to GECCO (Table 1) such that the net coast-to-coast STC convergence decreases by 8.5 Sv. In correspondence the EUC also shows a stronger decrease in the reference run, of 6.8 ± 3.5 Sv. These combined differences between the reference and the constrained model show again that the magnitude of the Ekman divergence changes determine what happens in the STC.

5. Summary and Concluding Remarks

[14] We analyze here the output fields from the German ECCO (GECCO) assimilation effort 1952–2002 with respect to the Subtropical Cell (STC) transports across 9°N and 9°S in the Pacific Ocean and their relation to changes of the Equatorial Undercurrent and eastern upwelling, and compare the constrained results to those available from the unconstrained reference run. Some of our main findings are:

[15] 1. The large multidecadal decreasing trend of the Ekman transport divergence across 9°N/9°S, amounting to about 20 Sv from the 1950's to the 1990's, as present in NCAR/NCEP wind stresses (Figure 4b), is largely eliminated in the GECCO wind estimates. This confirms earlier findings of *Alory et al.* [2005] that the NCEP trend in near-tropical zonal wind stress is unrealistically high and should have led to a large decadal change of zonal sea level

gradient which was not observed. It is interesting to note that the Ekman divergence of the constrained model adapts to the higher level of the 1960s instead of adjusting to the lower values of the better observed recent decade.

[16] 2. While the reference run yields a decrease of the interior STC convergence by about 10 Sv from the 1960s to the 1990s across 9°N/9°S, the assimilation reduces the decadal trend of the interior STC transport convergence to only about 5 Sv, about 40% of the amount estimated from hydrographic data analysis by MPZ (Figure 3b); the equivalent geostrophic STC convergence decrease (Figure 3b), when calculated as in MPZ, is only about 25% of their estimate. The SST increase of 0.6°C in the same time period is thus accompanied by a much smaller shallow overturning change than previously thought.

[17] 3. The STC varies mostly at interannual time scales, and an out-of-phase relation between the interior and wbc STC transports occurs, consistent with other model studies [*Lee and Fukumori*, 2003; *Capotondi et al.*, 2005; *Zhang and McPhaden*, 2006]. The interannual variability of the EUC is significantly correlated with the interior STC transport convergence, lagging by only several months.

[18] The cause of the discrepancy between the large STC convergence decline estimate of MPZ and the much lower one of the GECCO assimilation requires further study. GECCO, we have to remind ourselves, assimilates a much wider range of data than just the 9°N and 9°S sections as used by MPZ, and there must thus be other parts of the region where the slowdown is not occurring or much weaker than at those two selected sections, and GECCO adjusts to that. It should also be kept in mind, however, that the GECCO optimization is still not the final solution. Much has to be learned about data and model uncertainties before a fully consistent solution can be obtained. Moreover, the solution penalizes the drift of the model over the entire assimilation period. Some of that constraint, although imposed globally and not eliminating interdecadal changes
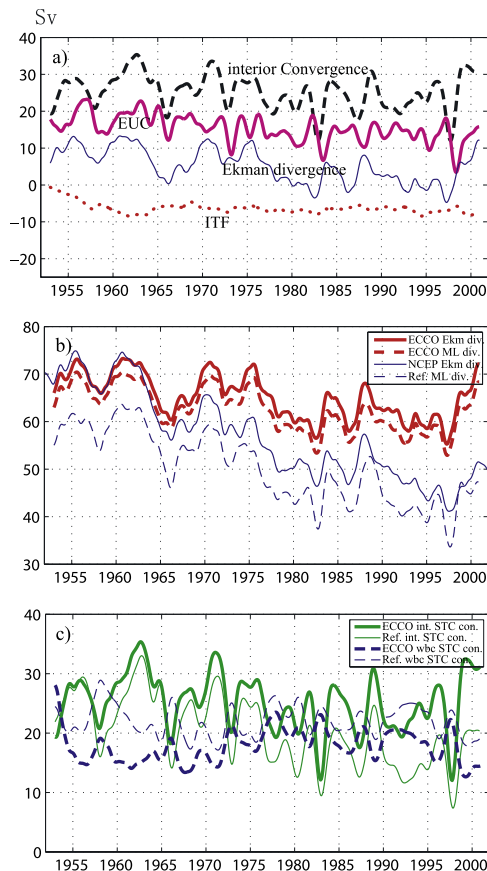
Figure 4. (a) Transports of the EUC at 140°W (heavy solid line), of interior STC convergence (dashed line) and Ekman divergence (add 60 Sv to l.h.s. scale) for 9°N/9°S sections from the stresses that GECCO produced by its assimilation process (thin solid line); also shown is transport of Indonesian Throughflow (ITF) in STC density range (dotted line); (b) Ekman transport divergence for 9°N/9°S sections, from GECCO (heavy solid line) and from NCEP wind stresses (thin solid line); also shown are mixed-layer ageostrophic (absolute minus geostrophic) transports from GECCO (heavy dashed line) and from the reference run (thin dashed line); (c) comparison of GECCO-wbc (heavy dashed line) and GECCO interior (heavy solid line) STC convergence with wbc STC convergence (thin dashed line) and interior STC convergence (thin solid line) from the reference run.

altogether, might suppress some of the observed interdecadal variability present. For a discussion of uncertainties of the GECCO solution we refer to *Köhl et al.* [2007] who provide a detailed discussion of remaining uncertainties of the ECCO solution which applies also to this GECCO solution.

References

Alory, G., S. Cravatte, T. Izumo, and K. B. Rogers (2005), Validation of a decadal OGCM simulation for the tropical Pacific, *Ocean Modell.*, *10*, 272–282.

Capotondi, A., M. A. Alexander, C. Deser, and M. J. McPhaden (2005), Anatomy and decadal evolution of the Pacific Subtropical-Tropical Cells (STCs), *J. Clim.*, *18*, 3739–3758.

Cheng, W., M. J. McPhaden, D. Zhang, and E. J. Metzger (2007), Recent changes in the Pacific subtropical cells inferred from an eddy resolving ocean circulation model, *J. Phys. Oceanogr*, in press.

Köhl, A., D. Dommenget, K. Ueyoshi, and D. Stammer (2006), The Global ECCO 1952 to 2001 ocean synthesis, *Rep..40*, Natl. Oceanogr. Partnership Program, Washington, D. C. (Available at http://www.ecco-group.org/ecco1/report/report_40.pdf)

Köhl, A., D. Stammer, and B. Cornuelle (2007), Interannual to decadal changes in the ECCO global synthesis, *J. Phys. Oceanogr*, *37*, 313–337.

Lee, T., and I. Fukumori (2003), Interannual-to-decadal variations of tropical-subtropical exchange in the Pacific Ocean: Boundary versus interior thermocline transports, *J. Clim.*, *16*, 4022–4042.

Malanotte-Rizzoli, P., K. Hedstrom, H. Arango, and D. B. Haidvogel (2000), Water mass pathways between the subtropical and tropical ocean in a climatological simulation of the North Atlantic Ocean circulation, *Dyn. Atmos. Oceans*, *32*, 331–371.

McCreary, J. P., Jr., and P. Lu (1994), Interaction between the subtropical and equatorial ocean circulations: The subtropical cell, *J. Phys. Oceanogr.*, *24*(2), 466–497.

McPhaden, M. J., and D. Zhang (2002), Slowdown of the meridional overturning circulation in the upper Pacific Ocean, *Nature*, *415*, 603–608.

McPhaden, M. J., and D. Zhang (2004), Pacific Ocean circulation rebounds, *Geophys. Res. Lett.*, *31*, L18301, doi:10.1029/2004GL020727.

Schott, F. A., J. P. McCreary, and G. C. Johnson (2004), Shallow overturning circulations of the tropical-subtropical oceans, in *Earth Climate: The Ocean-Atmosphere Interaction*, *Geophys. Monogr. Ser.*, vol. 147, edited by C. Wang, S.–P. Xie, and J. A. Carton, pp. 261–304, AGU, Washington, D. C.

Stammer, D., C. Wunsch, R. Giering, C. Eckert, P. Heimbach, J. Marotzke, A. Adcroft, C. N. Hill, and J. Marshall (2002), Global ocean circulation during 1992–1997, estimated from ocean observations and a general circulation model, *J. Geophys. Res.*, *107*(C9), 3118, doi:10.1029/2001JC000888.

Stammer, D., K. Ueyoshi, A. Köhl, W. B. Large, S. Josey, and C. Wunsch (2004), Estimating air-sea fluxes of heat, freshwater and momentum through global ocean data assimilation, *J. Geophys. Res.*, *109*, C05023, doi:10.1029/2003JC002082.

Zhang, D., and M. J. McPhaden (2006), Decadal variability of the shallow Pacific meridional overturning circulation: Relation to tropical sea surface temperatures in observations and climate change models, *Ocean Modell.*, *15*, 250–273.

————————————
F. Schott and W. Wang, Leibniz-Institut für Meereswissenschaften (IFM-GEOMAR), Düsternbrooker Weg 20, D-24105 Kiel, Germany. (fschott@ifm-geomar.de)

D. Stammer, Institut für Meereskunde, Zentrum für Marine und Atmosphärische Wissenschaften, Universität Hamburg, D-20146 Hamburg, Germany.